

OMEGA-Avatar: One-shot Modeling of 360° Gaussian Avatars

ZEHAO XIA, Chongqing University, China

YIQUN WANG, Chongqing University, China

ZHENGDA LU, University of Chinese Academy of Sciences, China

KAI LIU, Chongqing University, China

JUN XIAO, University of Chinese Academy of Sciences, China

PETER WONKA, KAUST, Saudi Arabia

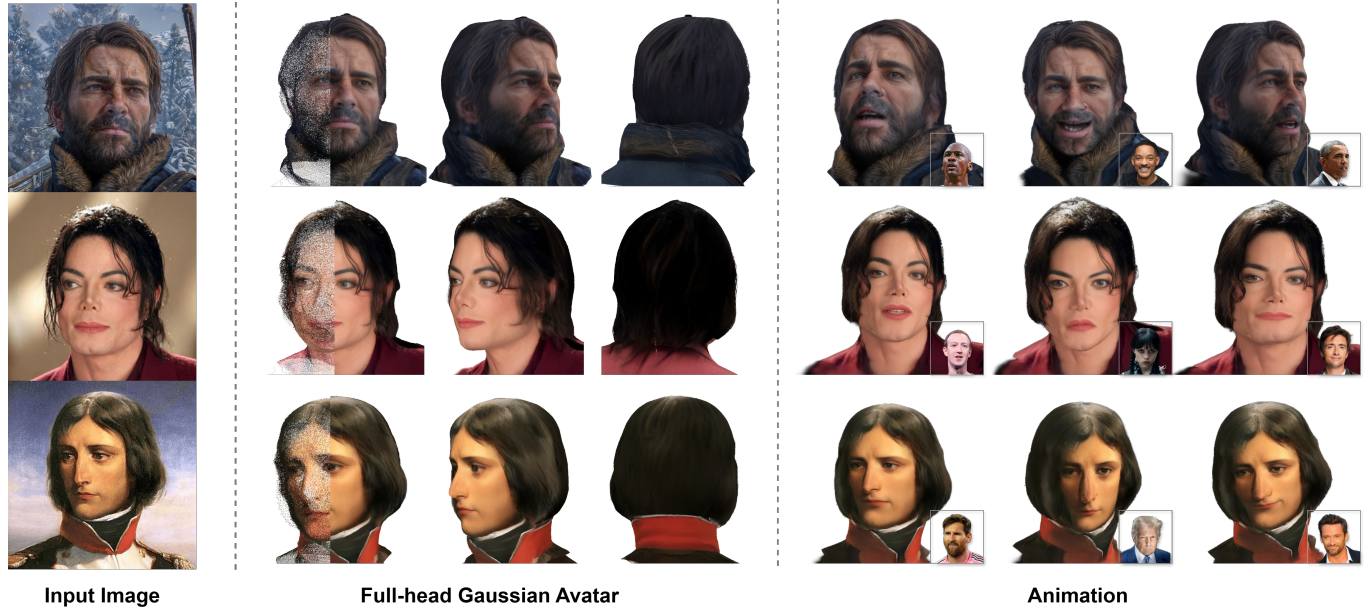


Fig. 1. Given a single portrait image across diverse styles (left), our method generates a high-fidelity Full-Head Gaussian avatar via a feed-forward network (middle). The reconstructed avatars include the back of the head and are capable of high-quality animations (right).

Creating high-fidelity, animatable 3D avatars from a single image remains a formidable challenge. We identified three desirable attributes of avatar generation: 1) the method should be feed-forward, 2) model a 360° full-head, and 3) should be animation-ready. However, current work addresses only two of the three points simultaneously. To address these limitations, we propose OMEGA-Avatar, the first feed-forward framework that simultaneously generates a generalizable, 360°-complete, and animatable 3D Gaussian head from a single image. Starting from a feed-forward and animatable framework, we address the 360° full-head avatar generation problem with two novel components. First, to overcome poor hair modeling in full-head avatar generation, we introduce a semantic-aware mesh deformation module that integrates multi-view normals to optimize a FLAME head with hair while preserving its topology structure. Second, to enable effective feed-forward decoding of full-head features, we propose a multi-view feature splatting module that constructs a shared canonical UV representation from features across multiple views through differentiable bilinear splatting, hierarchical UV mapping, and visibility-aware fusion. This approach preserves both global structural coherence and local high-frequency details across all viewpoints, ensuring 360° consistency without per-instance optimization. Extensive experiments demonstrate that OMEGA-Avatar achieves state-of-the-art performance, significantly outperforming existing baselines in 360° full-head completeness while preserving identity across different viewpoints.

Project Website: <https://omega-avatar.github.io/OMEGA-Avatar/>

CCS Concepts: • Computing methodologies → Reconstruction; Neural networks; Animation.

Additional Key Words and Phrases: Single-view Feed-forward Generation, Generalizable Full-head Avatars, Animation-ready, Gaussian Splatting

1 Introduction

Generating high-fidelity, animatable 3D full-head avatars from a single image is a pivotal challenge in computer graphics.

To make this severely under-constrained problem tractable in practice, we identified three essential properties that the avatar generator must possess: First, it should be feed-forward. Due to the under-constrained nature of single-image input, recovering a complete and animatable full-head avatar inevitably relies on strong learned priors from large-scale data. This makes a feed-forward formulation essential for generalizing across identities, in contrast to optimization-based approaches that require costly per-subject tuning. Second, it must support 360° full-head modeling. Unlike standard facial reconstruction, a complete avatar inferring

occluded geometry and appearance, such as hair and the back of the head, to ensure geometric completeness. This requirement typically demands multi-view supervision to hallucinate reasonable content in unseen regions. Third, the avatar should be animation-ready. Beyond static geometry, the model must support explicit control over expressions and poses. This capability relies on modeling additional motion-related information through a parametric model or video-based animation supervision, so that the reconstructed avatar can be consistently driven by explicit motion parameters while preserving identity.

However, satisfying all three attributes remains elusive.

Some generative approaches [1, 22, 40] leverage 3D-aware GANs or diffusion models to achieve 360° head synthesis. However, they lack explicit parametric head representations and remain constrained by inversion-based or sampling-heavy workflows, hindering efficient inference and animatable head generation. While FaceLift [28] attempts to generate animation frame-by-frame via diffusion, the stochastic nature of diffusion leads to temporal inconsistency and jittering. Methods like FATE [50] and SOAP [26] achieve animatable full heads by leveraging multi-view priors. However, both FATE and SOAP rely on instance-specific pipelines with costly optimization or remeshing. As a result, there is room to improve upon these methods in terms of efficiency and generalizability. Recent one-shot methods [6, 16] train feed-forward networks using large-scale 2D video datasets [43]. While they excel at frontal reenactment, they are unable to effectively decode full-head features in a feed-forward manner, leading to structural distortions when rendering side and back views and failing to generate 360° full-head avatars.

To bridge these gaps, we propose Ω -Avatar, the first feed-forward framework that generates a 360°-complete and animatable 3D avatar from a single image.

Within the feed-forward and animation-ready formulation, we propose two novel components for tackling full-head avatar generation as illustrated in Fig. 2. First, to address the difficulty of modeling complete head geometry under the constraint of limited 3D datasets, we leverage a pre-trained multi-view diffusion model to augment large-scale video data, producing consistent multi-view normal maps and RGB images without requiring multi-view capture. The synthesized normal maps are used as geometric priors to optimize a FLAME mesh with hair, enforcing cross-view consistency while preserving the underlying topology. Second, a key challenge lies in how to effectively fuse discrete and scale-inconsistent multi-view features into a unified representation suitable for feed-forward decoding. To this end, we propose a multi-view feature splatting mechanism that maps features from generated multiple views into a shared canonical UV space. This UV-based representation serves as a differentiable bridge, enabling robust aggregation of global structure and local high-frequency details across viewpoints. The resulting UV features are then decoded into 3D Gaussians and bound to the FLAME mesh via UV mapping. By jointly leveraging these two aspects, Ω -Avatar enables rapid generation of high-fidelity and animatable avatars without per-instance optimization.

Our main contributions are as follows:

- We propose the first feed-forward framework that enables the generation of generalizable, high-fidelity, full-head, and animatable avatars from a single image.

Table 1. Comparison of properties with state-of-the-art methods. Our method is the first to simultaneously achieve feed-forward, 360° full-head, and animatable avatar reconstruction from a single image.

Method	Representation	Feed-Forward	360° Full-Head	Animatable
Rodin [40]	Tri-plane	✓	✓	✗
PanoHead [1]	Tri-plane	✗*	✓	✗
SphereHead [22]	Tri-plane	✗*	✓	✗
FaceLift [15]	3DGS	✓	✓	✗
FATE [50]	3DGS	✗	✓	✓
GAGAvatar [6]	3DGS	✓	✗	✓
LAM [16]	3DGS	✓	✗	✓
SOAP [26]	Mesh	✗	✓	✓
Ours	3DGS	✓	✓	✓

* Denotes methods requiring per-instance GAN inversion prior to reconstruction.

- We introduce a multi-view feature splatting module, a fully differentiable multi-view feature fusion mechanism that constructs a shared canonical UV feature map from discrete 2D multi-view features for 3D Gaussian decoding.
- Extensive experiments demonstrate that our method achieves state-of-the-art performance on multi-view full-head generation, outperforming the main baseline (GAGAvatar) in both full-head completeness and multi-view visual fidelity on both datasets, with PSNR \uparrow 2.95%, SSIM \uparrow 0.30%, LPIPS \downarrow 7.39%, and DS \downarrow 8.03%.

2 Related work

Single-Image Head Avatar Reconstruction. Early 3DMM-based approaches [18, 44] provided strong statistical priors but often lacked fine-grained details. With the advent of Neural Radiance Fields [32] (NeRF), the field has shifted toward implicit representations, which offer higher fidelity in modeling complex attributes like hair [2, 19, 34, 53, 54]. Most NeRF-based methods rely on identity-specific multi-view or video data, limiting generalization to unseen subjects and raising privacy concerns. To avoid large-scale video data, generative approaches [5, 13, 33] and 3D-aware GANs like EG3D [4] achieve high visual quality via efficient tri-plane representations. Reconstructing specific identities requires costly latent inversion [37, 42], which often degrades accuracy and fails to fully preserve identity. Addressing the limitations of data requirements and computational cost, recent works have focused on one-shot 3D head reconstruction [7, 10, 11, 20, 24, 25, 27, 29, 30, 39, 45–48, 52]. 3D Gaussian Splatting (3DGS) [17] offers photorealistic rendering at real-time speeds, recent one-shot single-image adaptations [6, 16], represent significant progress. However, these methods often deteriorate in performance when rendered from diverse viewpoints, meaning they are not pure 3D solutions. Our work addresses these shortcomings by proposing a robust framework for one-shot 3D single-image animation that maintains high rendering efficiency and geometric consistency.

Generative Full-Head Reconstruction. Recent full-head modeling methods increasingly rely on generative models for novel view synthesis. GAN-based approaches [1, 22] enable high-quality 360° head synthesis via specialized volumetric representations. Diffusion-based approaches [40, 49] generate triplane head representations but remain static and unsuitable for animation.

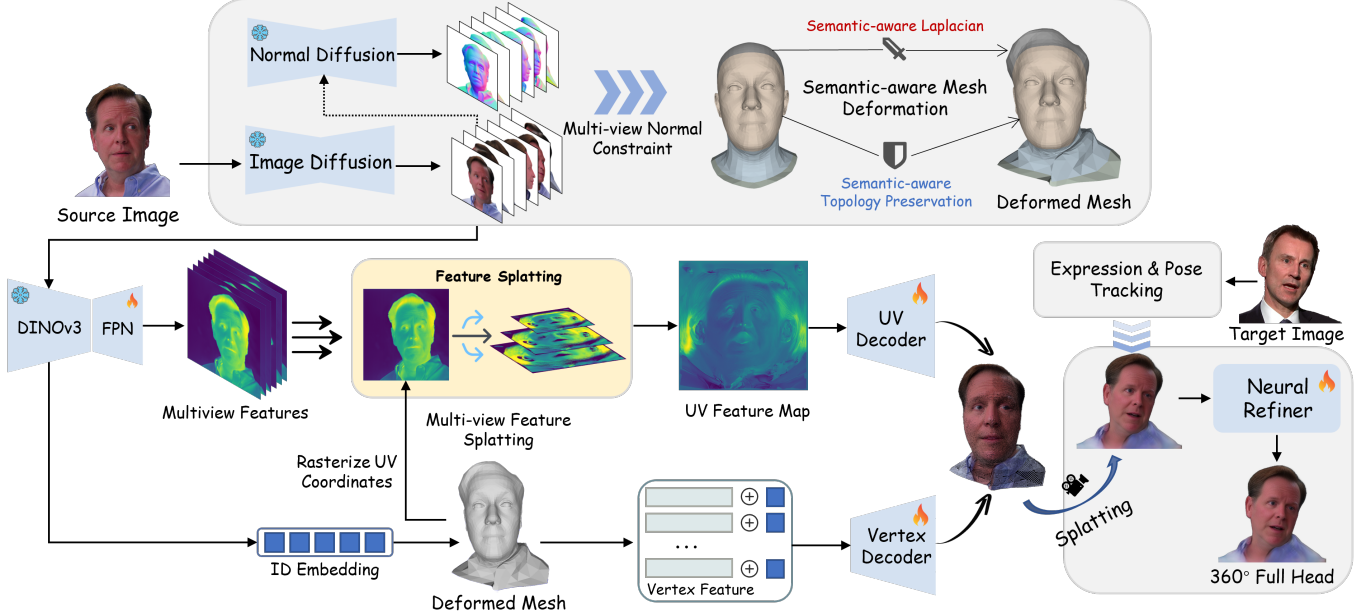


Fig. 2. Pipeline Overview. Given the source and target images, we leverage diffusion models to synthesize multi-view RGB images and corresponding normal maps. These normal maps are used to semantic-aware mesh deformation, while pixel-wise features are extracted from multi-view RGB images. Multi-view features are subsequently aggregated into a canonical UV feature map through the multi-view feature splatting module. The UV features and vertex features extracted from the deformed mesh are decoded and anchored to the mesh via UV mapping. For animation, the expression and pose derived from the target image are injected into the deformed mesh. Finally, the rendered output is enhanced by a neural refiner to generate the final full-head avatar.

SOAP [26] introduces a style-omniscient framework but relies on costly multi-stage remeshing and direct FLAME vertex optimization, which alters topology and degrades expression driving. To address these limitations, we present a novel framework capable of efficient, one-shot full-head reconstruction that supports high-quality animation.

3 Methodology

3.1 Overview

We present a framework for generating high-fidelity, animatable full-head Gaussian avatars from a single image, as illustrated in Fig. 2. We leverage diffusion models to generate RGB images and normal maps, which guide the semantic-aware deformation of a FLAME mesh to obtain a personalized mesh. Our approach employs a dual-branch architecture to generate Gaussians that construct the 3D representation. The UV Gaussian branch encodes appearance details; we employ DINOv3 [38] with a Feature Pyramid Network (FPN) to extract pixel-aligned features that fuse deep semantics with high-frequency geometric details. These multi-view features are aggregated into a unified UV feature map via splatted UV feature map module. The vertex Gaussian branch anchors Gaussians directly to the FLAME vertices to ensure structural coherence.

Finally, the Gaussians from two branches are driven by the underlying FLAME, which is deformed by target expression parameters and refined by a neural renderer to yield final outputs.

In the following subsections. Sec. 3.2 describes the process of semantic-aware mesh deformation. Sec. 3.3 elaborates on the canonical full-head avatar construction, introducing the specifics of both the UV and vertex Gaussian branches. Finally, the training strategy and losses are presented in Sec. 3.4.

3.2 Semantic-aware Mesh Deformation.

We leverage the pretrained diffusion model from SOAP [26], which builds upon the Unique3D [41] framework, to synthesize six RGB images I_{rgb} and normal maps I_{nml} from input.

Given the generated multi-view consistent normal maps I_{nml} and facial landmarks detected using [3], we aim to reconstruct a personalized mesh while maintaining a clean topology suitable for animation. Unlike previous FLAME tracking methods [36] that rely solely on landmarks or single-view photometric constraints, our approach is supervised by multi-view consistent normal maps. This rich geometric prior allows us to recover intricate 3D details that are typically lost in parametric fitting. To recover the personalized geometry, we propose a single-stage optimization framework. In contrast to prior art [26] that require multi-stage iterative remeshing to handle deformations, our method efficiently deforms the mesh in a single pass. We initialize the mesh using the FLAME template and introduce a deformation field. Let $\mathcal{M}(\beta, \theta, \psi)$ denote the standard FLAME driven by shape β , pose θ , and expression ψ . We optimize a per-vertex offset $\Delta V \in \mathbb{R}^{N \times 3}$ to capture high-frequency geometric details, where N denotes the number of vertices. Deformed vertices

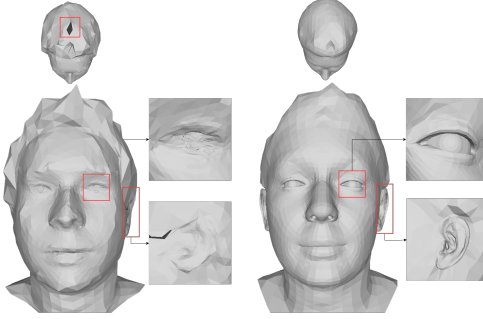


Fig. 3. Semantic-aware Mesh Deformation. Direct optimization with normal guidance disrupts the parametric structure of FLAME, causing severe surface irregularities and topological artifacts (left). Note the holes in the cranial region and the degeneration of facial features such as the eyes and ears (highlighted in red boxes). Our approach (right) mitigates these issues by incorporating semantic-aware topology preservation and a semantic-aware Laplacian. We preserve the clean topology of FLAME and ensure 360° geometric consistency, enabling the generation of fine details without compromising facial structural integrity.

\mathbf{V}' are formulated as:

$$\mathbf{V}' = \mathcal{M}(\beta, \theta, \psi) + \Delta\mathbf{V}. \quad (1)$$

Semantic-aware Topology Preservation. A core challenge in mesh deformation is balancing geometric fidelity with animatability. Unconstrained optimization of $\Delta\mathbf{V}$ across the entire mesh often disrupts the inherent semantic topology of the FLAME, leading to degraded expression reenactment quality. To address this, we introduce a semantic-aware optimization strategy. Specifically, we utilize a semantic mask to restrict the scope of the normal-guided deformation. We apply the normal consistency constraints strictly to the non-facial regions while preserving the parametric structure of the facial region. This design disentangles the optimization of static geometry from dynamic facial components, ensuring high-fidelity animation.

To ensure the deformation is both accurate and topologically coherent, we optimize $\Delta\mathbf{V}$ by minimizing the following composite objective function:

$$\mathcal{L} = \lambda_{nml}\mathcal{L}_{nml} + \lambda_{lmk}\mathcal{L}_{lmk} + \lambda_{lap}\mathcal{L}_{lap}, \quad (2)$$

The primary supervision comes from the normal consistency loss \mathcal{L}_{nml} , which minimizes the L_2 distance between the rendered normal of the deformed mesh and the diffusion-predicted maps \mathbf{I}_{nml} . To ensure semantic alignment, we employ a landmark loss \mathcal{L}_{lmk} that penalizes the projection error of 3D facial landmarks and enforces symmetry in the canonical space.

Semantic-aware Laplacian. Although restricting normal constraints to non-facial regions helps preserve facial topology, the cranial region remains susceptible to surface irregularities and topological artifacts due to the lack of supervision from top-view, as illustrated in Fig. 3. Standard Laplacian regularization is insufficient here: applying a uniform weight strong enough to smooth the cranial artifacts would inadvertently over-smooth the facial features. To resolve this conflict, we introduce a semantic-aware Laplacian smoothing term \mathcal{L}_{lap} with a spatially-varying weighting scheme:

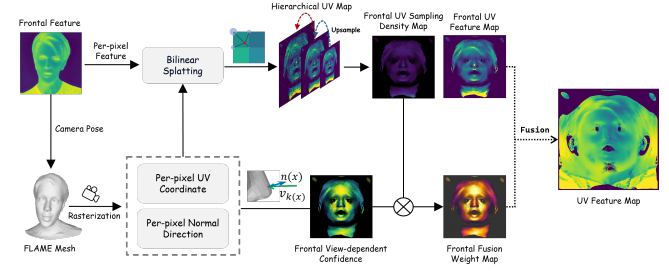


Fig. 4. Multi-view Feature Splatting. Taking a frontal view as an example, we first obtain per-pixel UV coordinates and normals via rasterization, and map features to UV space using differentiable bilinear splatting. We employ hierarchical UV mapping, which builds a multi-resolution pyramid to fill missing regions in a coarse-to-fine manner. Simultaneously, we calculate a fusion weight map by combining view-dependent confidence and UV sampling density. Finally, the visibility-aware fusion module aggregates the weighted features from all views to generate the final UV feature map.

$$\mathcal{L}_{lap} = \sum_{i=1}^N w_i \|\delta_i\|^2, \quad \delta_i = v'_i - \frac{1}{|N_{nei}(i)|} \sum_{j \in N_{nei}(i)} v'_j, \quad (3)$$

where δ_i is the Laplacian coordinate approximation for vertex i . Consistent with our semantic-aware strategy, the weight w_i is not constant; we assign significantly higher weights to the hair and boundary regions to suppress degeneration, while assigning minimal weights to the facial region. This ensures the cranium remains smooth without compromising the high-frequency details of the face preserved by the parametric prior.

3.3 Canonical Gaussian Full-head Avatar Generation

We model the canonical full-head avatar with a hybrid Gaussian representation that combines vertex Gaussians for expression control and UV Gaussians for view-consistent appearance modeling.

The vertex Gaussian Branch anchors 3D Gaussians to FLAME vertices to enable explicit expression driving. We extract a global identity token f_{id} from the frontal view, as it provides the most comprehensive identity information. Simultaneously, to distinguish different vertices and encode spatial details, we assign a unique learnable parameter to each vertex $v^{(i)}$. The global token is concatenated with these local parameters and fed into a vertex decoder to predict the Gaussian attributes $\mathcal{G}_{vert} = \{r^{(i)}, s^{(i)}, \alpha^{(i)}, c^{(i)}\}$. This design ensures geometric stability during animation.

While the vertex branch ensures structural stability, the limited number and discrete nature of FLAME vertices restrict vertex Gaussians from representing high-frequency details. To capture appearance while maintaining surface topological continuity, we introduce the UV Gaussian Branch. Given k generated multi-view images, we employ an image encoder to extract semantic feature maps \mathbf{F}_k . However, effectively aggregating feature maps from different views is non-trivial due to view-dependent variations and inconsistent feature scales across viewpoints. To achieve this, we propose a **Multi-view Feature Splatting** module that lifts multi-view 2D features onto a canonical UV map, enabling joint decoding of all

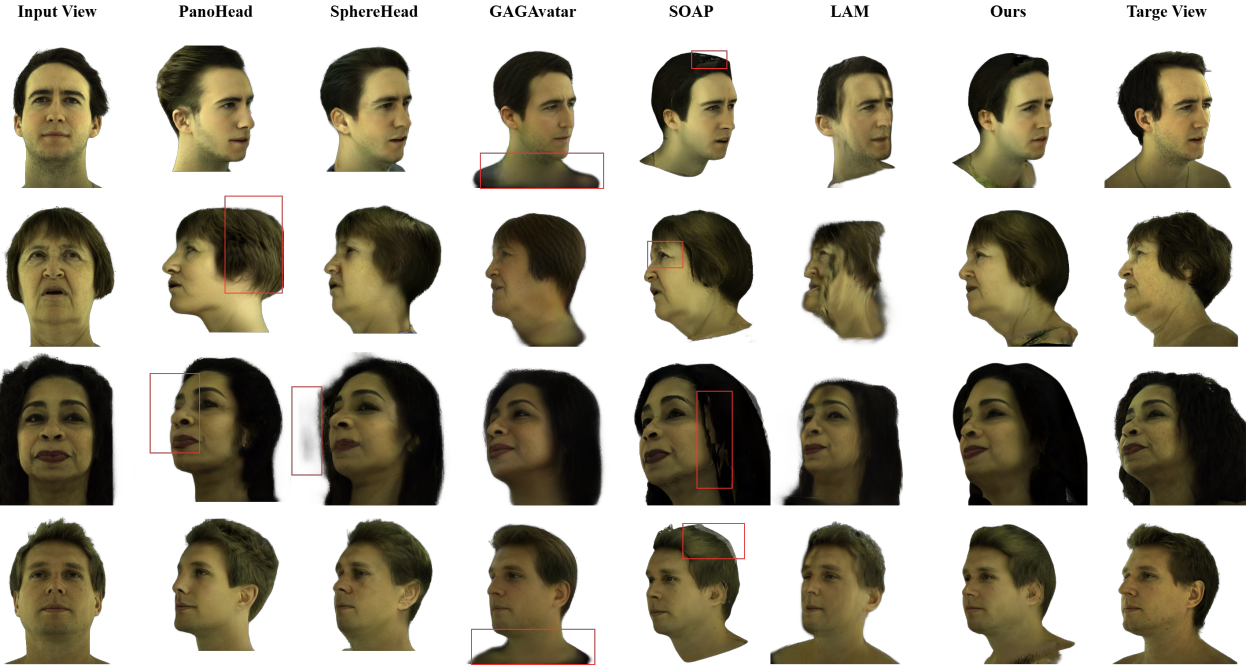


Fig. 5. **Novel view synthesis from single image on the Ava-256 dataset.** Compared to state-of-the-art methods, our approach better preserves identity consistency and high-quality rendering results, even under unseen and extreme side-view facial angles. Note that PanoHead and SphereHead require inputs aligned to the FFHQ canonical space, which leads to differences in apparent scale. We use the red boxes to highlight the visual artifacts.

views in a single pass. Our approach consists of three integral components: differentiable bilinear splatting, hierarchical UV mapping, and visibility-aware fusion, as shown in Fig. 4. This enables stable end-to-end gradient propagation from multi-view feature maps to the UV feature map.

Differentiable Bilinear Splatting. We first establish dense correspondences between screen pixels and UV coordinates. For a given view k with camera pose \mathbf{P}_k , we perform rasterization to retrieve a continuous UV coordinate $\mathbf{u}_p \in \mathbb{R}^2$ for each pixel p in the feature map. Direct nearest-neighbor assignment is prone to quantization artifacts. Instead, we adopt differentiable bilinear splatting and formulate it as a differentiable aggregation operator over the UV domain. Given a pixel feature \mathbf{f}_p and its continuous UV coordinate \mathbf{u}_p , bilinear splatting softly distributes the feature to neighboring UV grid locations according to a bilinear kernel induced by \mathbf{u}_p .

Aggregating contributions from all pixels yields a per-view UV feature map \mathbf{U}_k and a corresponding density map \mathbf{D}_k :

$$\mathbf{U}_k = \sum_p \mathcal{B}(\mathbf{u}_p) \mathbf{f}_p, \quad \mathbf{D}_k = \sum_p \mathcal{B}(\mathbf{u}_p), \quad (4)$$

where $\mathcal{B}(\mathbf{u}_p)$ denotes the bilinear splatting operator induced by \mathbf{u}_p . \mathbf{D}_k records the effective sampling density in the UV space.

Hierarchical UV Mapping. A critical challenge in splatting is the resolution mismatch between screen space and texture space, which often results in sparse coverage and "holes" in the UV map. To address this issue, we introduce a hierarchical UV map representation. Instead of splatting features only at the target UV resolution, we splat them onto a pyramid of UV maps with progressively lower

resolutions. At each pyramid level l , bilinear splatting produces a feature map $\mathbf{U}_{k,l}$, and an associated density map $\mathbf{D}_{k,l}$. To synthesize the final high-resolution map, we employ a coarse-to-fine hole-filling mechanism. Coarser UV maps, which possess broader receptive fields and denser coverage, are upsampled to the target resolution. We fuse these upsampled features with the finer-scale features using a soft, differentiable mask derived from the density map $\mathbf{D}_{k,l}$. Specifically, regions with low splatting density at the fine level are smoothly filled by the upsampled global context from coarser levels, effectively repairing artifacts without introducing discontinuities.

Visibility-aware Fusion.

After obtaining the completed UV feature maps from one view, we fuse the multi-view UV feature maps into a single canonical UV feature map. The fusion weight for each view is defined by combining three complementary factors.

View Weight: Since frontal views typically contain richer information, we assign each view a predefined global weight γ_k .

View-dependent Confidence: We define a view-dependent geometric confidence to measure the reliability of observations under a given view k . For each pixel p , the included angle between the surface normal \mathbf{n}_p and the viewing direction \mathbf{v}_k determines the reliability of the feature. We aggregate these per-pixel confidence scores into the UV domain using the same splatting operator:

$$\mathbf{C}_k = \sum_p \mathcal{B}(\mathbf{u}_p) \cdot \max(0, \mathbf{n}_p \cdot \mathbf{v}_k). \quad (5)$$

This naturally down-weights grazing-angle observations while preserving strong signals from front-facing surfaces.

Table 2. Quantitative Comparison of Novel View Synthesis on the Avatar-256 and NeRSemle Datasets. Colors denote the best and second-best

Method	Ava-256 Novel Views					NeRSemle Novel Views				
	PSNR \uparrow	SSIM \uparrow	LPIPS \downarrow	CSIM \uparrow	DS \downarrow	PSNR \uparrow	SSIM \uparrow	LPIPS \downarrow	CSIM \uparrow	DS \downarrow
PanoHead	17.995	0.5932	0.2592	0.4556	0.1663	17.151	0.6098	0.2706	0.5742	0.1082
SphereHead	18.932	0.6238	0.2436	0.4714	0.1509	17.446	0.6183	0.2628	0.5781	0.1053
GAGAvatar	22.802	0.7714	0.1719	0.4682	0.1762	22.556	0.8027	0.1505	0.6867	0.1033
SOAP	21.335	0.7287	0.1948	0.5783	0.1890	19.539	0.7471	0.1975	0.6855	0.1128
LAM	21.802	0.7314	0.1997	0.4842	0.1818	20.263	0.7465	0.1853	0.6321	0.1118
Ours	23.244	0.7734	0.1592	0.5403	0.1651	23.221	0.8051	0.1435	0.6714	0.0950

UV Sampling Density: The accumulated density $D_{k,l}$ reflects how many features contribute to a given UV coordinate at pyramid level l , serving as a measure of feature reliability. The final canonical UV feature map U is obtained by a globally normalized weighted average over all views k and pyramid levels l . We define the composite fusion weight map $W_{k,l}$ as the element-wise product of view weight γ_k , the geometric confidence C_k , and the sampling density $D_{k,l}$:

$$W_{k,l} = \gamma_k \cdot C_k \odot D_{k,l}. \quad (6)$$

Using these weights, the fused feature map is computed as:

$$U = \frac{\sum_k \sum_l W_{k,l} \odot U_{k,l}}{\sum_k \sum_l W_{k,l} + \epsilon}. \quad (7)$$

This formulation prioritizes densely observed and front-facing regions, while allowing coarser-scale features and alternative views to smoothly fill missing or weakly observed areas.

3.4 Training Strategy and Losses

We train the framework using a self-reenactment scheme, minimizing the discrepancy between the rendered output and the driving frame. The total objective function is a composite of reconstruction, perceptual, multi-view constraints and local regularization (details in Supplementary Material).

To balance 3D consistency and expression flexibility, we propose a progressive side-view decay strategy. Strong multi-view constraints are essential for full-head reconstruction but hinder expression learning, while weak constraints cause frontal overfitting. We therefore start training with a high λ_{mv} to stabilize canonical geometry, and gradually decay it to relax the constraints, enabling the avatar to learn high-frequency facial expressions while preserving underlying structure.

4 Experiments

4.1 Experimental Setting

Baselines and Evaluation Metric. We compare with five recent works: PanoHead [1], SphereHead [22], GAGAvatar [6], LAM [16], and SOAP [26]. PanoHead and SphereHead are state-of-the-art methods for 3D full-head reconstruction using 3D GANs. GAGAvatar and LAM are the one-shot animatable avatar reconstruction methods based on 3D Gaussian Splatting. SOAP is a diffusion-based method that reconstructs the full head by remeshing a FLAME mesh. We

employ five quantitative metrics. For reconstruction quality and perceptual fidelity, we report PSNR, SSIM, LPIPS [51], and DreamSim [12]. To evaluate identity preservation, we report CSIM, which computes cosine similarity of face recognition features extracted using ArcFace [9].

4.2 Main Results

To evaluate our method’s 3D consistency and novel view synthesis capabilities, we leverage two publicly available multi-view datasets: NeRSemle [21] and Avatar-256 [31]. For both datasets, reconstruction is performed from a single input image, while multi-view observations are used only for evaluation; full details of the dataset splits, view selection, and camera settings are provided in the supplementary material. Furthermore, to demonstrate generalization in unconstrained scenarios, we collect a set of in-the-wild face images for qualitative assessment.

Qualitative results. Fig. 5 presents a qualitative comparison between our method and baselines under novel viewpoints. Unlike competing approaches, our method synthesizes photorealistic 3D renderings while maintaining consistency in fine-grained details and identity, even under extreme viewpoint variations. In contrast, PanoHead and SphereHead struggle to preserve identity across views, suffering from severe identity-view ambiguity. Constrained by single-view training data and the lack of 3D priors, GAGAvatar and LAM frequently exhibit structural distortions at large viewing angles. Regarding the mesh-based SOAP, its remeshing process is prone to surface fragmentation, leading to visible artifacts. Consequently, our approach demonstrates superior robustness, simultaneously ensuring identity preservation, and high-fidelity details.

Quantitative results. Tab. 2 reports quantitative results on the NeRSemle and Avatar-256 datasets, respectively. In terms of visual fidelity, our method demonstrates superior rendering quality as evidenced by the PSNR, SSIM, LPIPS, and DreamSim (DS) metrics, while maintaining strong identity consistency with high CSIM scores. Regarding reconstruction efficiency, PanoHead and SphereHead necessitate a time-consuming Pivotal Tuning Inversion process to optimize latent codes; SOAP relies on a multi-stage remeshing process for each subject; GAGAvatar, LAM, and our method all employ feed-forward networks for 3D Gaussian prediction, the former two baselines lack multi-view priors, resulting in suboptimal

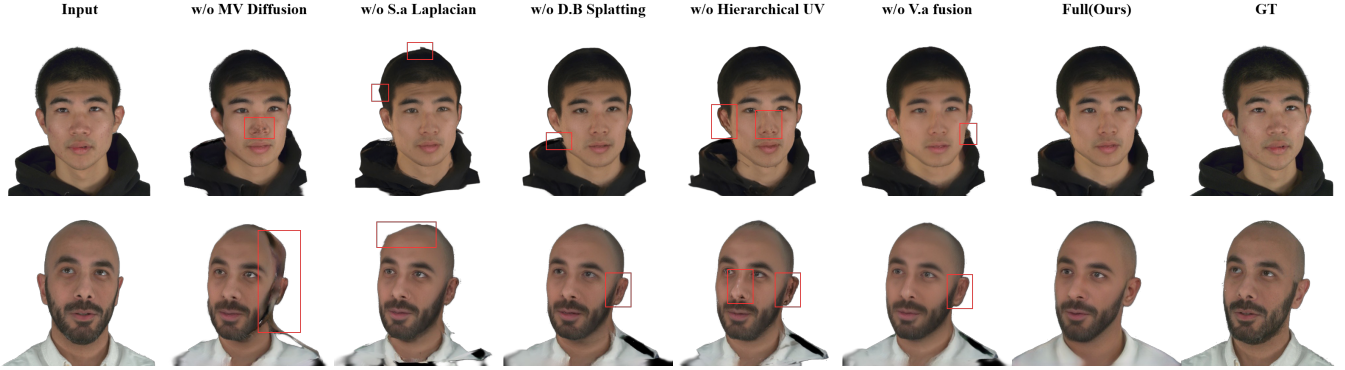


Fig. 6. **Qualitative Ablation on the NeRSemle dataset.** We compare results for models trained: (1) without multi-view diffusion, (2) without using semantic-aware Laplacian term, (3) without differentiable bilinear splatting, (4) without hierarchical UV mapping, (5) without visibility-aware fusion.

performance on multi-view datasets compared to our approach. Ultimately, our method realizes genuine one-shot, animatable full-head reconstruction, achieving state-of-the-art performance on both the NeRSemle and Avatar-256 benchmarks.

Results on In-the-wild Images. To further evaluate the generalization capability, we collected a set of in-the-wild facial images. Fig. 7 presents qualitative comparisons against baseline methods in these unconstrained scenarios. PanoHead and SphereHead often fail to accurately reconstruct complex hairstyles. GAGAvatar and LAM suffer from severe structural distortions in back and side views. While SOAP recovers accurate global geometry, it frequently manifests visible cracks in the back of the head due to mesh fragmentation. These results collectively demonstrate the robust generalization and superior full-head reconstruction capabilities of our method.

Table 3. **Ablation of different components on the NeRSemle dataset.**

Method	Ablation Novel Views				
	PSNR \uparrow	SSIM \uparrow	LPIPS \downarrow	CSIM \uparrow	DS \downarrow
Single view	22.687	0.774	0.151	0.655	0.124
w/o S.a Laplacian	22.988	0.782	0.150	0.667	0.105
w/o D.B Splatting	23.187	0.789	0.141	0.643	0.098
w/o Hierarchical UV	22.997	0.785	0.149	0.655	0.103
w/o V.a fusion	23.121	0.793	0.151	0.597	0.110
Full (Ours)	23.221	0.805	0.144	0.671	0.095

4.3 Ablation Studies

We conduct ablation studies on single-view reconstruction using the NeRSemle dataset. The quantitative and qualitative results are presented in Tab. 3 and Fig. 6, respectively.

w/o MV Diffusion. We remove the multi-view diffusion step. Significant artifacts appear at the rendering boundaries of the frontal view. Furthermore, the synthesis quality for side and rear views degrades drastically, failing to reconstruct a complete, animatable 3D avatar. This confirms the necessity of diffusion-based priors for hallucinating unobserved geometry and texture.

w/o Semantic-aware Laplacian. We remove the semantic-aware Laplacian constraint. As shown in Fig. 6, this leads to geometric inconsistencies. The rendering fidelity decreases, with noticeable surface irregularities emerging along the head and facial contours, resulting in bumpy geometry, indicating that the Laplacian term is crucial for maintaining surface smoothness and mesh integrity.

w/o Differentiable Bilinear Splatting. We replace our differentiable bilinear splatting with a hard nearest-neighbor assignment and fix the density weights to 1. Although the LPIPS metric shows a slight improvement—likely due to the absence of interpolation blur—all other quantitative metrics decline. Qualitatively, the lack of differentiable gradients and soft distribution leads to quantization artifacts and a loss of fine-grained details in the rendered results.

w/o Hierarchical UV Mapping. We disable the hierarchical pyramid and splat features onto a fixed-resolution UV map. As observed in Fig. 6, this results in significant blurring in areas like the nose and ears. The mismatch between the feature map resolution and the UV grid causes "holes" in the UV feature space, thereby degrading the decoding capability and expressiveness of the Gaussian primitives.

w/o Visibility-aware Fusion. We remove the view-dependent weights, relying solely on UV sampling density for aggregation. As reported in Table 3, the CSIM score drops significantly, indicating a loss of identity preservation. Visually, prominent artifacts appear around the nasal bridge, where lower-quality features from oblique side views override the high-fidelity information from the frontal view. This demonstrates that visibility-aware weighting is essential for correctly prioritizing high-confidence observations.

5 Conclusion

We presented Ω -Avatar, the first feed-forward framework that reconstructs generalizable, full-head, and animatable 3D avatars from a single image. By introducing a semantic-aware mesh deformation module that integrates multi-view normals to optimize a haired FLAME head, together with a multi-view feature splatting module that aggregates full-head features into a shared canonical UV representation, our method enables effective feed-forward decoding of complete head geometry, offering a robust solution for efficient 3D avatar creation.

References

[1] Sizhe An, Hongyi Xu, Yichun Shi, Guoxian Song, Umit Y. Ogras, and Linjie Luo. 2023. PanoHead: Geometry-Aware 3D Full-Head Synthesis in 360deg. In *Proceedings of the IEEE/CVF Conference on Computer Vision and Pattern Recognition (CVPR)*. 20950–20959.

[2] Yunpeng Bai, Yanbo Fan, Xuan Wang, Yong Zhang, Jingxiang Sun, Chun Yuan, and Ying Shan. 2023. High-fidelity Facial Avatar Reconstruction from Monocular Video with Generative Priors. In *IEEE/CVF Conference on Computer Vision and Pattern Recognition, CVPR 2023, Vancouver, BC, Canada, June 17–24, 2023*. IEEE, 4541–4551. [doi:10.1109/CVPR52729.2023.00041](https://doi.org/10.1109/CVPR52729.2023.00041)

[3] Adrian Bulat and Georgios Tzimiropoulos. 2017. How Far are We from Solving the 2D & 3D Face Alignment Problem? (and a Dataset of 230, 000 3D Facial Landmarks). In *IEEE International Conference on Computer Vision, ICCV 2017, Venice, Italy, October 22–29, 2017*. IEEE Computer Society, 1021–1030. [doi:10.1109/ICCV.2017.116](https://doi.org/10.1109/ICCV.2017.116)

[4] Eric R. Chan, Connor Z. Lin, Matthew A. Chan, Koki Nagano, Boxiao Pan, Shalini De Mello, Orazio Gallo, Leonidas J. Guibas, Jonathan Tremblay, Sameh Khamis, Tero Karras, and Gordon Wetzstein. 2022. Efficient Geometry-aware 3D Generative Adversarial Networks. In *IEEE/CVF Conference on Computer Vision and Pattern Recognition, CVPR 2022, New Orleans, LA, USA, June 18–24, 2022*. IEEE, 16102–16112. [doi:10.1109/CVPR52688.2022.01565](https://doi.org/10.1109/CVPR52688.2022.01565)

[5] Eric R. Chan, Marco Monteiro, Petr Kellnhofer, Jiajun Wu, and Gordon Wetzstein. 2021. Pi-GAN: Periodic Implicit Generative Adversarial Networks for 3D-Aware Image Synthesis. In *IEEE Conference on Computer Vision and Pattern Recognition, CVPR 2021, virtual, June 19–25, 2021*. Computer Vision Foundation / IEEE, 5799–5809. [doi:10.1109/CVPR46437.2021.00574](https://doi.org/10.1109/CVPR46437.2021.00574)

[6] Xuangeng Chu and Tatsuya Harada. 2024. Generalizable and Animatable Gaussian Head Avatar. In *Advances in Neural Information Processing Systems 38: Annual Conference on Neural Information Processing Systems 2024, NeurIPS 2024, Vancouver, BC, Canada, December 10 – 15, 2024*.

[7] Xuangeng Chu, Yu Li, Ailing Zeng, Tianyu Yang, Lijian Lin, Yunfei Liu, and Tatsuya Harada. 2024. GPAvatar: Generalizable and Precise Head Avatar from Image(s). In *The Twelfth International Conference on Learning Representations, ICLR 2024, Vienna, Austria, May 7–11, 2024*. OpenReview.net.

[8] Radek Danecek, Michael J. Black, and Timo Bolkart. 2022. EMOCA: Emotion Driven Monocular Face Capture and Animation. In *IEEE/CVF Conference on Computer Vision and Pattern Recognition, CVPR 2022, New Orleans, LA, USA, June 18–24, 2022*. IEEE, 20279–20290. [doi:10.1109/CVPR52688.2022.01967](https://doi.org/10.1109/CVPR52688.2022.01967)

[9] Jiankang Deng, Jia Guo, Jing Yang, Niannan Xue, Irene Kotsia, and Stefanos Zafeiriou. 2022. ArcFace: Additive Angular Margin Loss for Deep Face Recognition. *IEEE Trans. Pattern Anal. Mach. Intell.* 44, 10 (2022), 5962–5979. [doi:10.1109/TPAMI.2021.3087709](https://doi.org/10.1109/TPAMI.2021.3087709)

[10] Yu Deng, Duomin Wang, Xiaohang Ren, Xingyu Chen, and Baoyuan Wang. 2024. Portrait4D: Learning One-Shot 4D Head Avatar Synthesis using Synthetic Data. In *IEEE/CVF Conference on Computer Vision and Pattern Recognition*.

[11] Yu Deng, Duomin Wang, and Baoyuan Wang. 2024. Portrait4D-V2: Pseudo Multi-view Data Creates Better 4D Head Synthesizer. In *Computer Vision - ECCV 2024 - 18th European Conference, Milan, Italy, September 29–October 4, 2024, Proceedings, Part XVII (Lecture Notes in Computer Science, Vol. 15075)*. Springer, 316–333. [doi:10.1007/978-3-031-72643-9_19](https://doi.org/10.1007/978-3-031-72643-9_19)

[12] Stephanie Fu, Netanel Tamir, Shobhita Sundaram, Lucy Chai, Richard Zhang, Tali Dekel, and Phillip Isola. 2023. DreamSim: Learning New Dimensions of Human Visual Similarity using Synthetic Data. In *Advances in Neural Information Processing Systems 36: Annual Conference on Neural Information Processing Systems 2023, NeurIPS 2023, New Orleans, LA, USA, December 10 – 16, 2023*.

[13] Jiajiao Gu, Lingjie Liu, Peng Wang, and Christian Theobalt. 2022. StyleNeRF: A Style-based 3D Aware Generator for High-resolution Image Synthesis. In *The Tenth International Conference on Learning Representations, ICLR 2022, Virtual Event, April 25–29, 2022*. OpenReview.net.

[14] Jianzhu Guo, Xiangyu Zhu, and Zhen Lei. 2018. 3DDFA. <https://github.com/cleardusk/3DDFA>.

[15] Yue Han, Junwei Zhu, Keke He, Xu Chen, Yanhao Ge, Wei Li, Xiangtai Li, Jiangning Zhang, Chengjie Wang, and Yong Liu. 2024. Face-Adapter for Pre-trained Diffusion Models with Fine-Grained ID and Attribute Control. In *Computer Vision - ECCV 2024 - 18th European Conference, Milan, Italy, September 29–October 4, 2024, Proceedings, Part L (Lecture Notes in Computer Science, Vol. 15108)*. Springer, 20–36. [doi:10.1007/978-3-031-72973-7_2](https://doi.org/10.1007/978-3-031-72973-7_2)

[16] Yisheng He, Xiaodong Gu, Xiaodan Ye, Chao Xu, Zhengyi Zhao, Yuan Dong, Weihao Yuan, Zilong Dong, and Liefeng Bo. 2025. LAM: Large Avatar Model for One-shot Animatable Gaussian Head. *CoRR* abs/2502.17796 (2025). [doi:10.48550/ARXIV.2502.17796](https://doi.org/10.48550/ARXIV.2502.17796)

[17] Bernhard Kerbl, Georgios Kopanas, Thomas Leimkühler, and George Drettakis. 2023. 3D Gaussian Splatting for Real-Time Radiance Field Rendering. *ACM Trans. Graph.* 42, 4 (2023), 139:1–139:14. [doi:10.1145/3592433](https://doi.org/10.1145/3592433)

[18] Taras Khakhulin, Vanessa Sklyarova, Victor Lempitsky, and Egor Zakharov. 2022. Realistic One-Shot Mesh-Based Head Avatars. In *Computer Vision - ECCV 2022 - 17th European Conference, Tel Aviv, Israel, October 23–27, 2022, Proceedings, Part II (Lecture Notes in Computer Science, Vol. 13662)*. Springer, 345–362. [doi:10.1007/978-3-031-20086-1_20](https://doi.org/10.1007/978-3-031-20086-1_20)

[19] Taekyung Ki, Dongchan Min, and Gyeongsu Chae. 2024. Learning to Generate Conditional Tri-plane for 3D-aware Expression Controllable Portrait Animation. *arXiv preprint arXiv:2404.00636* (2024).

[20] Tobias Kirschstein, Simon Gibebnain, Jiapeng Tang, Markos Georgopoulos, and Matthias Nießner. 2024. GGHead: Fast and Generalizable 3D Gaussian Heads. In *SIGGRAPH Asia 2024 Conference Papers, SA 2024, Tokyo, Japan, December 3–6, 2024*, Takeo Igarashi, Ariel Shamir, and Hao (Richard) Zhang (Eds.). ACM, 126:1–126:11. [doi:10.1145/3680528.3687686](https://doi.org/10.1145/3680528.3687686)

[21] Tobias Kirschstein, Shenhuan Qian, Simon Gibebnain, Tim Walter, and Matthias Nießner. 2023. NeRSeble: Multi-view Radiance Field Reconstruction of Human Heads. *ACM Trans. Graph.* 42, 4 (2023), 161:1–161:14. [doi:10.1145/3592455](https://doi.org/10.1145/3592455)

[22] Heyuan Li, Ce Chen, Tianhao Shi, Yuda Qiu, Sizhe An, Guanying Chen, and Xiaoguang Han. 2024. SphereHead: Stable 3D Full-Head Synthesis with Spherical Tri-Plane Representation. In *Computer Vision - ECCV 2024 - 18th European Conference, Milan, Italy, September 29–October 4, 2024, Proceedings, Part LXXV, Vol. 15133*, 324–341. [doi:10.1007/978-3-031-73226-3_19](https://doi.org/10.1007/978-3-031-73226-3_19)

[23] Tianyue Li, Timo Bolkart, Michael J. Black, Hao Li, and Javier Romero. 2017. Learning a model of facial shape and expression from 4D scans. *ACM Transactions on Graphics (Proc. SIGGRAPH Asia)* 36, 6 (2017), 194:1–194:17.

[24] Weichuang Li, Longhao Zhang, Dong Wang, Bin Zhao, Zhigang Wang, Mulin Chen, Bang Zhang, Zhongjian Wang, Liefeng Bo, and Xuelong Li. 2023. One-Shot High-Fidelity Talking-Head Synthesis with Deformable Neural Radiance Field. In *IEEE/CVF Conference on Computer Vision and Pattern Recognition, CVPR 2023, Vancouver, BC, Canada, June 17–24, 2023*. IEEE, 17969–17978. [doi:10.1109/CVPR52729.2023.01723](https://doi.org/10.1109/CVPR52729.2023.01723)

[25] Xueteng Li, Shalini De Mello, Sifei Liu, Koki Nagano, Umar Iqbal, and Jan Kautz. 2023. Generalizable One-shot 3D Neural Head Avatar. In *Advances in Neural Information Processing Systems 36: Annual Conference on Neural Information Processing Systems 2023, NeurIPS 2023, New Orleans, LA, USA, December 10 – 16, 2023*, Alice Oh, Tristan Naumann, Amir Globerson, Kate Saenko, Moritz Hardt, and Sergey Levine (Eds.).

[26] Tingting Liao, Yujian Zheng, Adilbek Karmanov, Liwen Hu, Leyang Jin, Yuliang Xiu, and Hao Li. 2025. SOAP: Style-Omniscient Animatable Portraits. *CoRR* abs/2505.05022 (2025). [doi:10.48550/ARXIV.2505.05022](https://doi.org/10.48550/ARXIV.2505.05022)

[27] Xin Lu, Chuanqing Zhuang, Chenxi Jin, Zhengda Lu, Yiqun Wang, Wu Liu, and Jun Xiao. 2025. LSF-Animation: Label-Free Speech-Driven Facial Animation via Implicit Feature Representation. *CoRR* abs/2510.21864 (2025). [doi:10.48550/ARXIV.2510.21864](https://doi.org/10.48550/ARXIV.2510.21864)

[28] Weijie Lyu, Yi Zhou, Ming-Hsuan Yang, and Zhixin Shu. 2025. FaceLift: Learning Generalizable Single Image 3D Face Reconstruction from Synthetic Heads. In *Proceedings of the IEEE/CVF International Conference on Computer Vision (ICCV)*, 12691–12701.

[29] Haoyu Ma, Tong Zhang, Shanlin Sun, Xiangyi Yan, Kun Han, and Xiaohui Xie. 2024. CTVHead: One-shot Controllable Head Avatar with Vertex-feature Transformer. In *IEEE/CVF Winter Conference on Applications of Computer Vision, WACV 2024, Waikoloa, HI, USA, January 3–8, 2024*. IEEE, 6119–6129. [doi:10.1109/WACV57701.2024.00602](https://doi.org/10.1109/WACV57701.2024.00602)

[30] Zhiyuan Ma, Xiangyu Zhu, Guojun Qi, Zhen Lei, and Lei Zhang. 2023. OTAvatar: One-Shot Talking Face Avatar with Controllable Tri-Plane Rendering. In *IEEE/CVF Conference on Computer Vision and Pattern Recognition, CVPR 2023, Vancouver, BC, Canada, June 17–24, 2023*. IEEE, 16901–16910. [doi:10.1109/CVPR52729.2023.01621](https://doi.org/10.1109/CVPR52729.2023.01621)

[31] Juliette Martinez, Emily Kim, Javier Romero, Timur M. Bagautdinov, Shunsuke Saito, Shouo-I Yu, Stuart Anderson, Michael Zollhöfer, Te-Li Wang, Shaojie Bai, Chenghui Li, Shih-En Wei, Rohan Joshi, Wyatt Borsos, Tomas Simon, Jason M. Saragih, Paul Theodosis, Alexander Greene, Anjani Josyula, Silvio Maeta, Andrew Jewett, Simion Vensthai, Christopher Heilmann, Yueh-Tung Chen, Sidi Fu, Mohamed Elshaer, Tingfang Du, Longhua Wu, Shen-Chi Chen, Kai Kang, Michael Wu, Youseff Emad, Steven Longay, Ashley Brewer, Hitesh Shah, James Booth, Taylor Koska, Kayla Haidle, Matthew Andromalos, Joanna Hsu, Thomas Dauer, Peter Selednik, Timothy Godisar, Scott Ardisson, Matthew Cipperly, Ben Humberston, Lon Farr, Bob Hansen, Peihong Guo, Dave Braun, Steven Krenn, He Wen, Lucas Evans, Natalia Fadueva, Matthew Stewart, Gabriel Schwartz, Divam Gupta, Gyeongsik Moon, Kaiwen Guo, Yuan Dong, Yichen Xu, Takaaki Shiratori, Fabian Prada, Bernardo Pires, Bo Peng, Julia Buffalini, Autumn Trimble, Kevyn McPhail, Melissa Schoeller, and Yaser Sheikh. 2024. Codec Avatar Studio: Paired Human Captures for Complete, Driveable, and Generalizable Avatars. In *Advances in Neural Information Processing Systems 38: Annual Conference on Neural Information Processing Systems 2024, NeurIPS 2024, Vancouver, BC, Canada, December 10 – 15, 2024*.

[32] Ben Mildenhall, Pratul P. Srinivasan, Matthew Tancik, Jonathan T. Barron, Ravi Ramamoorthi, and Ren Ng. 2020. NeRF: Representing Scenes as Neural Radiance Fields for View Synthesis. In *Computer Vision - ECCV 2020 - 16th European Conference, Glasgow, UK, August 23–28, 2020, Proceedings, Part I (Lecture Notes in Computer Science, Vol. 12346)*. Springer, 405–421. [doi:10.1007/978-3-030-58452-8_24](https://doi.org/10.1007/978-3-030-58452-8_24)

[33] Roy Or-El, Xuan Luo, Mengyi Shan, Eli Shechtman, Jeong Joon Park, and Ira Kemelmacher-Shlizerman. 2022. StyleSDF: High-Resolution 3D-Consistent Image and Geometry Generation. In *IEEE/CVF Conference on Computer Vision and Pattern Recognition, CVPR 2022, New Orleans, LA, USA, June 18-24, 2022*. IEEE, 13493–13503. [doi:10.1109/CVPR52688.2022.01314](https://doi.org/10.1109/CVPR52688.2022.01314)

[34] Keunhong Park, Utkarsh Sinha, Jonathan T. Barron, Sofien Bouaziz, Dan B. Goldman, Steven M. Seitz, and Ricardo Martin-Brualla. 2021. Nerfies: Deformable Neural Radiance Fields. In *2021 IEEE/CVF International Conference on Computer Vision, ICCV 2021, Montreal, QC, Canada, October 10-17, 2021*. IEEE, 5845–5854. [doi:10.1109/ICCV48922.2021.00581](https://doi.org/10.1109/ICCV48922.2021.00581)

[35] Omkar Parkhi, Andrea Vedaldi, and Andrew Zisserman. 2015. Deep face recognition. In *BMVC 2015-Proceedings of the British Machine Vision Conference 2015*. British Machine Vision Association.

[36] Shenhan Qian. 2024. VHAP: Versatile Head Alignment with Adaptive Appearance Priors. [doi:10.5281/zenodo.14988309](https://doi.org/10.5281/zenodo.14988309)

[37] Daniel Roich, Ron Mokady, Amit H. Bermano, and Daniel Cohen-Or. 2023. Pivotal Tuning for Latent-based Editing of Real Images. *ACM Trans. Graph.* 42, 1 (2023), 6:1–6:13. [doi:10.1145/3544777](https://doi.org/10.1145/3544777)

[38] Oriane Siméoni, Huy V. Vo, Maximilian Seitzer, Federico Baldassarre, Maxime Oquab, Cijo Jose, Vasil Khalidov, Marc Szafraniec, Seung Eun Yi, Michaël Ramamrisona, Francisco Massa, Daniel Haziza, Luca Wehrstedt, Jianyuan Wang, Timothée Darce, Théo Moutakanni, Leonel Sentana, Claire Roberts, Andrea Vedaldi, Jamie Tolan, John Brandt, Camille Couprie, Julien Mairal, Hervé Jégou, Patrick Labatut, and Piotr Bojanowski. 2025. DINOV3. *CoRR* abs/2508.10104 (2025). [doi:10.48550/ARXIV.2508.10104](https://doi.org/10.48550/ARXIV.2508.10104)

[39] Phong Tran, Egor Zakharov, Long-Nhat Ho, Anh Tuan Tran, Liwen Hu, and Hao Li. 2024. VOODOO 3D: Volumetric Portrait Disentanglement for One-Shot 3D Head Reenactment. In *Proceedings of the IEEE/CVF Conference on Computer Vision and Pattern Recognition*.

[40] Tengfei Wang, Bo Zhang, Ting Zhang, Shuyang Gu, Jianmin Bao, Tadas Baltrusaitis, Jingjin Shen, Dong Chen, Fang Wen, Qifeng Chen, and Baining Guo. 2023. RODIN: A Generative Model for Sculpting 3D Digital Avatars Using Diffusion. In *IEEE/CVF Conference on Computer Vision and Pattern Recognition, CVPR 2023, Vancouver, BC, Canada, June 17-24, 2023*. IEEE, 4563–4573. [doi:10.1109/CVPR52729.2023.00443](https://doi.org/10.1109/CVPR52729.2023.00443)

[41] Kailu Wu, Fangfu Liu, Zhihan Cai, Runjie Yan, Hanyang Wang, Yating Hu, Yueqi Duan, and Kaisheng Ma. 2024. Unique3D: High-Quality and Efficient 3D Mesh Generation from a Single Image. In *Advances in Neural Information Processing Systems 38: Annual Conference on Neural Information Processing Systems 2024, NeurIPS 2024, Vancouver, BC, Canada, December 10 - 15, 2024*.

[42] Jiaxin Xie, Hao Ouyang, Jingtan Piao, Chenyang Lei, and Qifeng Chen. 2023. High-fidelity 3D GAN Inversion by Pseudo-multi-view Optimization. In *IEEE/CVF Conference on Computer Vision and Pattern Recognition, CVPR 2023, Vancouver, BC, Canada, June 17-24, 2023*. IEEE, 321–331. [doi:10.1109/CVPR52729.2023.00039](https://doi.org/10.1109/CVPR52729.2023.00039)

[43] Liangbin Xie, Xintao Wang, Honglun Zhang, Chao Dong, and Ying Shan. 2022. VFHQ: A High-Quality Dataset and Benchmark for Video Face Super-Resolution. In *The IEEE Conference on Computer Vision and Pattern Recognition Workshops (CVPRW)*.

[44] Sicheng Xu, Jiaolong Yang, Dong Chen, Fang Wen, Yu Deng, Yunde Jia, and Xin Tong. 2020. Deep 3D Portrait From a Single Image. In *2020 IEEE/CVF Conference on Computer Vision and Pattern Recognition, CVPR 2020, Seattle, WA, USA, June 13-19, 2020*. Computer Vision Foundation / IEEE, 7707–7717. [doi:10.1109/CVPR42600.2020.00773](https://doi.org/10.1109/CVPR42600.2020.00773)

[45] Songlin Yang, Wei Wang, Yushi Lan, Xiangyu Fan, Bo Peng, Lei Yang, and Jing Dong. 2024. Learning Dense Correspondence for NeRF-Based Face Reenactment. In *Thirty-Eighth AAAI Conference on Artificial Intelligence, AAAI 2024, Thirty-Sixth Conference on Innovative Applications of Artificial Intelligence, IAAI 2024, Fourteenth Symposium on Educational Advances in Artificial Intelligence, EAAI 2024, February 20-27, 2024, Vancouver, Canada*. AAAI Press, 6522–6530. [doi:10.1609/AAAI.V38I7.28473](https://doi.org/10.1609/AAAI.V38I7.28473)

[46] Xin Yao, Junyi He, Chang Li, Yang Xie, Haotian Luo, Wei Zheng, Hongxing Qin, and Yiqun Wang. 2025. JFG-HMR: 3D joint feature-guided human mesh recovery with global-local feature fusion. *Comput. Graph.* 132 (2025), 104339. [doi:10.1016/J.CAG.2025.104339](https://doi.org/10.1016/J.CAG.2025.104339)

[47] Zhenhui Ye, Tianyun Zhong, Yi Ren, Jiaqi Yang, Weichuang Li, Jiawei Huang, Ziyue Jiang, Jinzheng He, Rongjie Huang, Jinglin Liu, Chen Zhang, Xiang Yin, Zejun Ma, and Zhou Zhao. 2024. Real3D-Portrait: One-shot Realistic 3D Talking Portrait Synthesis. In *The Twelfth International Conference on Learning Representations, ICLR 2024, Vienna, Austria, May 7-11, 2024*. OpenReview.net.

[48] Wangbo Yu, Yanbo Fan, Yong Zhang, Xuan Wang, Fei Yin, Yunpeng Bai, Yan-Pei Cao, Ying Shan, Yang Wu, Zhongqian Sun, and Baoyuan Wu. 2023. NOFA: NeRF-based One-shot Facial Avatar Reconstruction. In *ACM SIGGRAPH 2023 Conference Proceedings, SIGGRAPH 2023, Los Angeles, CA, USA, August 6-10, 2023*, Erik Brunvand, Alla Sheffer, and Michael Wimmer (Eds.). ACM, 85:1–85:12. [doi:10.1145/3588432.3591555](https://doi.org/10.1145/3588432.3591555)

[49] Bowen Zhang, Yiji Cheng, Chunyu Wang, Ting Zhang, Jiaolong Yang, Yansong Tang, Feng Zhao, Dong Chen, and Baining Guo. 2024. RodinHD: High-Fidelity 3D Avatar Generation with Diffusion Models. In *Computer Vision - ECCV 2024 - 18th European Conference, Milan, Italy, September 29-October 4, 2024, Proceedings, Part XIV (Lecture Notes in Computer Science, Vol. 15072)*. Springer, 465–483. [doi:10.1007/978-3-031-72630-9_27](https://doi.org/10.1007/978-3-031-72630-9_27)

[50] Jiawei Zhang, Zijian Wu, Zhiyang Liang, Yicheng Gong, Dongfang Hu, Yao Yao, Xun Cao, and Hao Zhu. 2025. FATE: Full-head Gaussian Avatar with Textural Editing from Monocular Video. In *IEEE/CVF Conference on Computer Vision and Pattern Recognition, CVPR 2025, Nashville, TN, USA, June 11-15, 2025*. Computer Vision Foundation / IEEE, 5535–5545. [doi:10.1109/CVPR52734.2025.00520](https://doi.org/10.1109/CVPR52734.2025.00520)

[51] Richard Zhang, Phillip Isola, Alexei A. Efros, Eli Shechtman, and Oliver Wang. 2018. The Unreasonable Effectiveness of Deep Features as a Perceptual Metric. In *2018 IEEE Conference on Computer Vision and Pattern Recognition, CVPR 2018, Salt Lake City, UT, USA, June 18-22, 2018*. Computer Vision Foundation / IEEE Computer Society, 586–595. [doi:10.1109/CVPR.2018.00068](https://doi.org/10.1109/CVPR.2018.00068)

[52] Shikun Zhang, Cunjian Chen, Yiqun Wang, QiuHong Ke, and Yong Li. 2025. EAvatar: Expression-Aware Head Avatar Reconstruction with Generative Geometry Priors. *CoRR* abs/2508.13537 (2025). [doi:10.48550/ARXIV.2508.13537](https://doi.org/10.48550/ARXIV.2508.13537)

[53] Yufeng Zheng, Wang Yifan, Gordon Wetzstein, Michael J. Black, and Otmar Hilliges. 2023. PointAvatar: Deformable Point-Based Head Avatars from Videos. In *IEEE/CVF Conference on Computer Vision and Pattern Recognition, CVPR 2023, Vancouver, BC, Canada, June 17-24, 2023*. IEEE, 21057–21067. [doi:10.1109/CVPR52729.2023.02017](https://doi.org/10.1109/CVPR52729.2023.02017)

[54] Wojciech Zienolka, Timo Bolkart, and Justus Thies. 2023. Instant Volumetric Head Avatars. In *IEEE/CVF Conference on Computer Vision and Pattern Recognition, CVPR 2023, Vancouver, BC, Canada, June 17-24, 2023*. IEEE, 4574–4584. [doi:10.1109/CVPR52729.2023.00444](https://doi.org/10.1109/CVPR52729.2023.00444)



Fig. 7. Additional Results on In-the-wild Images. Our method demonstrates great generalization ability and robustness towards in-the-wild images, and provides realistic unseen view rendering results. We use the red boxes to highlight the visual artifacts.

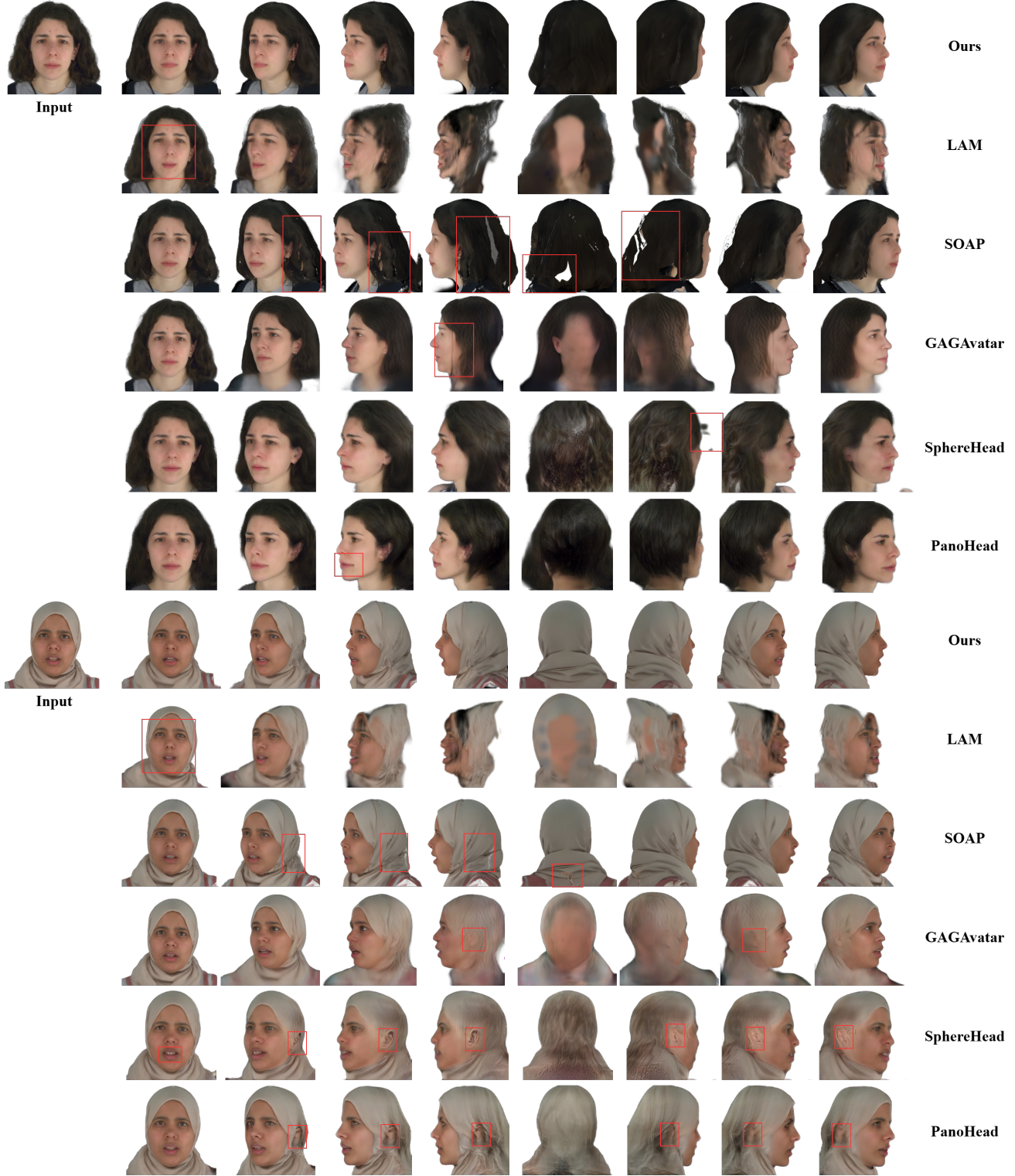


Fig. 8. More Visual results on NeRSemble dataset. Taking a single view as input, we perform 360° novel view synthesis to compare our method with state-of-the-art approaches. The results show that our method achieves superior multi-view consistency and accurately reconstructs unseen regions. We use the red boxes to highlight the visual artifacts.

Supplementary Material

A ...

In this supplementary material, we present additional results and implementation details of our method. In Section A, we elaborate on the training framework. Section B details the expression reenactment pipeline. We then describe the specific experimental settings in Section C. Section D presents additional results on novel view synthesis and 360° full-head reconstruction.

B Training Details

To achieve high-fidelity reenactment with robust geometry, our optimization is guided by a composite objective function comprising reconstruction, perceptual, and multi-view consistency terms. First, to ensure pixel-level photometric consistency, we employ an L_1 reconstruction loss \mathcal{L}_{rec} . This is applied to both the raw splatted image I_{raw} and the final neural-refined image I_{ref} . To further enhance high-frequency details in critical facial areas, we incorporate a bounding-box loss \mathcal{L}_{box} on the cropped facial region:

$$\mathcal{L}_{rec} = |I_{raw} - I_d| + |I_{ref} - I_d| + \lambda_{box} \mathcal{L}_{box}, \quad (8)$$

To preserve high-level facial identity and structural semantics, we incorporate a perceptual loss \mathcal{L}_{perc} derived from a pre-trained face recognition network [35]. Then, to alleviate depth ambiguity and enforce 3D geometric consistency, we introduce a pseudo-multi-view supervision \mathcal{L}_{mv} . We leverage the diffusion-generated multi-view data as pseudo-ground truth. Crucially, this supervision is restricted to the raw render result I_{raw} , ensuring geometric constraints while avoiding overfitting of the neural refiner to potential artifacts. Finally, we impose regularization terms \mathcal{L}_{local} on the local position offsets and scaling attributes of the UV Gaussians to prevent the UV Gaussians from drifting away from the underlying surface. The total objective function is formulated as:

$$\mathcal{L} = \mathcal{L}_{rec} + \lambda_{perc} \mathcal{L}_{perc} + \lambda_{mv} \mathcal{L}_{mv} + \lambda_{local} \mathcal{L}_{local}, \quad (9)$$

where the λ terms are hyperparameters that balance the contributions.

Training Datasets. We utilize the FFHQ dataset [43] for training, which comprises high-quality video clips from various interview scenarios. To ensure data diversity and avoid consecutive redundancy, we sample 25 to 75 frames per clip depending on its length, resulting in a total of 571951 frames from 15,204 video clips. All images are resized to 512 × 512. Following [6], we remove the background and track camera poses and FLAME [23] parameters for each frame. Crucially, to bridge the gap between monocular observations and 3D supervision, we employ our pre-trained diffusion model to expand these monocular frames into pseudo-multi-view data, which provide the necessary geometric and appearance constraints for training.

Implementation Details. Our framework is implemented on the PyTorch platform. We employ FLAME [23] as our driving 3DMM. For feature extraction, we utilize DINOv3 [38] as the backbone network, which remains frozen during the entire training process. To enable multi-view supervision, we preprocess the FFHQ dataset by generating multi-view images for each frame using a pre-trained diffusion model. These generated pseudo-multi-views are then utilized

as ground truth for supervision during training. We use the Adam [Kingma and Ba, 2014] optimizer with a learning rate of 1.0×10^{-4} . The model is trained for 250,000 iterations with a batch size of 6 on two NVIDIA H100 GPUs.

C Expression Reenactment

The goal of Expression Reenactment is to transfer the pose and expression from a driving image to the source image while preserving the source identity and maintaining high fidelity. After decoding, the Gaussian primitives from the vertex and UV branches are combined to form a complete canonical 3D Gaussian avatar. To animate this avatar, we first employ a face tracker [8] to extract the expression and pose parameters from the driving image. These parameters are then injected into the canonical avatar via the FLAME, explicitly driving the Gaussians to the target state. Finally, the deformed Gaussians are rendered using the camera parameters of the driving view via splatting.

D Experimental Details

We evaluate our method leverage two publicly available multi-view datasets: NeRSemle [21] and Avatar-256 [31].

NeRSemle dataset The NeRSemle dataset consists of 425 identities, each captured by 16 fixed cameras. For quantitative evaluation, we randomly sampled 10 identities and selected 9 sequences for each identity. From each sequence, we further randomly sampled 50 frames. For every frame, we utilize camera 222200037 as the single input view, as it represents the dataset-defined frontal perspective, while the remaining camera views serve as the test views. The specific identities used for evaluation are listed in Tab. 4.

Ava-256 dataset The Ava-256 dataset consists of 256 identities, each captured by 80 cameras, with over 5,000 frames per camera. For qualitative evaluation, we randomly sampled 10 identities and selected 20 random frames from the 5,000 available frames for each identity. For each selected frame, we use camera 401168 as the single input view. This camera is selected for its frontal perspective and central position in the world coordinate system, while the remaining views are reserved for testing. The specific identities used for evaluation are listed in Tab. 4.

For PanoHead [1] and SphereHead [22], we apply 3DDFA-V2 [14] to align the input image to the FFHQ canonical space. The aligned image is then inverted using Pivotal Tuning Inversion [37] for single-view head reconstruction.

For the remaining methods, we strictly follow their official implementations to obtain the target-view camera parameters, and render the output by rotating the camera to the target view.

E MORE RECONSTRUCTION RESULTS

We provide additional visual results of our method. Fig. 9 presents additional qualitative results of our method on the NeRSemle and Avatar-256 datasets for novel view synthesis, while Fig. 10 presents more results of our model on in-the-wild data, demonstrating 360° full-head reconstruction.

Table 4. Identities used from the NeRSemble and Ava-256 datasets.

Index	NeRSemble ID	Ava-256 ID
1	017	20220614-1135-DNM410
2	070	20220808-0809-DPE040
3	124	20230308-1352-BDF920
4	175	20230328-0800-BLY735
5	214	20230405-1635-AAN112
6	218	20230726-1657-AYE877
7	304	20230728-0757-CRV122
8	306	20230810-1355-AJR151
9	371	20230901-1429-CPP930
10	490	20230908-1645-DHA971



Fig. 9. Additional qualitative results on the NeRSemble and Avatar-256 datasets. We use the red boxes to highlight the visual artifacts.



Fig. 10. Full-head reconstruction results on in-the-wild images

, Vol. 1, No. 1, Article . Publication date: February 2026.